IEEE Access
Multidisciplinary | Rapid Review | Open Access Journal

Received December 17, 2018, accepted January 14, 2019, date of publication January 25, 2019, date of current version February 12, 2019.

Digital Object Identifier 10.1109/ACCESS.2019.2895131

Indoor Localization Using Visible Light via Two-Layer Fusion Network

XIANSHENG GUO[1,2], (Member, IEEE), FANGZI HU[1], (Student Member, IEEE), NKROW RAPHAEL ELIKPLIM[1], AND LIN LI[1], (Student Member, IEEE)

[1]Department of Electronic Engineering, University of Electronic Science and Technology of China, Chengdu 611731, China
[2]Wuhu Overseas Students Pioneer Park, Wuhu 241006, China

Corresponding author: Xiansheng Guo (xsguo@uestc.edu.cn)

This work was supported in part by the National Natural Science Foundation of China under Grant 61371184, Grant 61671137, Grant 61771114, and Grant 61771316, and in part by the Application Foundation Projects of the Science and Technology Department in Sichuan Province under Grant 2018JY0242 and Grant 2018JY0218.

ABSTRACT In visible light communication (VLC)-based indoor localization environment, the instability and uncertainty power of emitting LEDs and other factors, as obstacles between transmitters and receivers, will lead the fluctuation of the received signal strength of receivers. To overcome the problem, this paper proposes a two-layer fusion network (TLFN) indoor localization method for VLC. The two layers in TLFN are the diverse layer and the fusion layer. In the diverse layer, TLFN obtains multiple position estimates based on the predictions of multiple fingerprints and multiple classifiers combinations. In the fusion layer, TLFN first trains and stores some weights for all grid points by minimizing the average localization errors overall fingerprints and classifiers spaces. Then, in the online phase, we propose an optimal weights searching algorithm to intelligently determine the optimal weights for fusion localization. TLFN can leverage the intrinsic supplementation among multiple position estimates to yield a higher accurate positioning result. The experiments conducted on an intensity-modulated direct detection system demonstrate that our proposed TLFN is superior to existing fusion-based approaches regardless of the instability and uncertainty power of light-emitting-diode localization environments.

INDEX TERMS Indoor positioning, received signal strength (RSS), two-layer fusion network (TLFN), visible light communication (VLC).

I. INTRODUCTION

Indoor positioning employing light-emitting-diode (LED) has become a hot topic in wireless communications. Compared to other traditional positioning systems like WiFi and Ultra-Wideband (UWB) which require extra equipments installation and are also sensitive to RF-banned areas, VLC-based localization has the following but not limited advantages: cost efficiency, broad bandwidth, energy efficiency and communication security [1], [2]. It is obvious that indoor localization using VLC has become an effective alternative to conventional positioning technologies [3], especially with WiFi being very prominent like the works in [4]–[6].

Most prevalent localization schemes in VLC-based positioning first extract the relevant parameters from the received VLC signal and then utilize them for position estimation [7]–[9]. Common positioning algorithms include proximity-based methods, geometric methods, statistical methods, and fingerprint methods. Among them, fingerprint-based methods have attracted more attention because their more auspicious than the other three methods in complicated or dynamic environments. Regarding localization techniques, a variety of positioning parameters have been studied including time of arrival (TOA) [10], [11], time difference of arrival (TDOA) [12], angle of arrival (AOA) [13] and received signal strength (RSS) [14], [15]. Among these technologies, TOA requires accurate time synchronization between transmitters and receivers and may increase cost significantly. TDOA is an alternative approach to TOA, and this method only needs synchronization between LED transmitters instead of the requirement of time critical synchronization between LEDs and receivers. AOA achieves a fairly high accuracy, but it is susceptible to external environments and needs an antenna array. Compared to other characteristics of transmitted signals, RSS is easy to obtain without the need of auxiliary devices, and thus has gained popularity as the

mainstream positioning technology in VLC-based localization recently.

Based on the heuristics of the above references, we propose a novel fusion-based localization scheme known as two-layer fusion networks (TLFN). TLFN fuses multiple positioning estimates (MPEs) generated by multiple fingerprints and multiple classifiers under supervised learning mechanism. Unlike traditional fusion schemes, TLFN first constructs a diverse layer which amalgamates the advantages of diverse fingerprints and classifiers. Considering that no particular fingerprint or classifier is the global optimal, we harness the fact that each unique fingerprint depicts the environmental information from disparate perspectives or stances. In addition, to further excavate the intrinsic correlation of location estimates obtained from the diverse layer, we utilize the fusion layer to dynamically combine the outputs based on a trained FP in the offline phase. Finally, an optimal weights searching (OWS) strategy is designed to search the optimal weights for fusion.

- Our proposed TLEN-based VLC localization framework can obtain high accuracy without knowing the powers of the transmitters as well as the locations of these transmitters, and is thus robust to the uncertainty power of transmitters.
- A TLFN-based VLC localization framework is proposed in this work. As compared to conventional fingerprint-level fusion methods [4], [16], [17] and algorithm-level fusion methods [5], [14], [18], [19], our proposed fusion scheme combines the merits of the two praxis to yield a more accurate positioning estimate. Our proposed localization framework is more robust to the fluctuations of transmitter power hiccup.
- The proposed diverse layer in TLFN consists of multiple fingerprint-classifier combinations, where each modality can produce one estimation of position using their own knowledge. These diversified location estimates provide the potential to enhance positioning accuracy via amalgamating them together.
- The proposed fusion layer in TLFN generates an aggregated location estimation, accurate than the estimation made by utilizing a single fingerprint-classifier pair. This combination eliminates or reduces the risk of being stuck in the local optimal.

The rest of the paper is organized as follows: Related works are discussed in Section II. Section III introduces the proposed VLC-based signal model and localization framework. Our proposed TLFN-based fusion localization algorithm is presented in Section IV, where we introduce the implementation of the fusion network including diverse layer and fusion layer. Section V illustrates the experimental setup and analyzes the proposed algorithm's performance. Some conclusions are drawn in Section VI.

II. RELATED WORKS

Transmitters may vary regarding emitting power, resulting in changes in RSS values, ultimately affect positioning accuracy [20]. To overcome the variances in RSS, many fusion-based solutions have been proposed and proved their superiority in the application of indoor localization like [14] and [16]–[19]. Most existing fusion-based positioning schemes can be categorized into fingerprint-level fusion methods [16], [17] and algorithm-level fusion methods [14], [18], [19]. The former approach focuses on the amalgamation of multiple fingerprints, where each fingerprint excavates environmental information from its own perspective. Specifically, Fang and Wang proposed a delta-fused principal strength which embeds discriminative power within ΔRSS [16], and the proposed positioning feature achieves better computational efficiency. Guo *et al.* first proposed a novel fingerprints framework by fusing a group of fingerprints (GOOF) in [17], which includes RSS, signal subspace, covariance matrix, fractional low-order moment and fourth-order cumulant via multiple antennas in the offline stage. Similarly, Guo *et al.* [4], utilized RSS, hyperbolic location fingerprint (HLF) [21] and signal strength difference (SSD) [22] to generate a WiFi-based GOOF for more accurate localization results. Similar to the fingerprint-level fusion methods, the algorithm-level fusion methods combine the merits of multiple positioning algorithms. Gwon *et al.* [18] proposed a selective fusion location estimation strategy by considering location information from triangulation, K-nearest neighbor (KNN) and smallest M-vertex polygon. Moreover, machine learning based fusion methods have attracted much attention, since they outperform the traditional RSS-based approaches in positioning accuracy or robustness [5], [14], [19]. So far, machine learning based fusion methods have been rarely utilized in VLC-based positioning, but they have been extensively exploited in WiFi, ZigBee and other radio frequency networks.

Existing fusion-based approaches provide possibilities to excavate complementary advantages between multiple fingerprints/algorithms via weighting strategy. There are two main weighting strategies to compute the fusion profile (FP) used to store weight: one is the supervised learning mechanism [4], [5], [14], [23] which trains fusion weights through labeled data in the offline phase; the other is the unsupervised learning mechanism which derives weights directly without the need of an offline data [18]. Given a comprehensive training data, the former scheme shows better performance than the latter method since it considers the weights of diverse fingerprints/algorithms.

Different from the above methods, we propose a two-layer fusion network (TLFN) for visible light localization, which can fully leverage all the advantages of multiple fingerprints and multiple algorithms because our method has a bigger fusion space than those of most existing fusion works.

III. SIGNAL MODEL AND LOCALIZATION FRAMEWORK

A. SIGNAL MODEL

The configuration of our indoor VLC-based system is shown in Fig. 1. The LEDs are located at known locations as separate

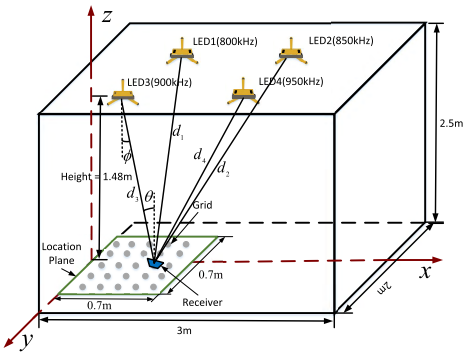

FIGURE 1. The configuration of our VLC-based positioning system.

transmitters, where each LED is modulated using an on-off-keying (OOK) to generate a unique identification code for distinguishing its position. Based on the received signals, a photo dioxide (PD) receiver can derive its distances to each LED and determine its position.

Consider a VLC-based positioning system with N LED transmitters at known locations $\boldsymbol{p}_i = [x_i, y_i, o_i]^T$ and a removable PD receiver at an unknown location $\boldsymbol{p} = [x, y, o]^T$. We transmit N different sinusoidal signals $s_i(l)$ with different frequencies f_i from N LEDs, and the received signal $\gamma(l)$ by the PD receiver at time index l is given by Eq. (1).

$$\gamma(l) = \sum_{i=1}^{N} \alpha_i \beta_i s_i(l - \tau_i) + n(l), \tag{1}$$

where α_i stands for the attenuation factor between the i-th LED and the receiver, β_i represents the conversion factor from the optical to the electrical domain and $n(l)$ is the noise. Note that α_i is real and positive [10] and it can further be formulated as Eq. (2) based on a generalized Lambertian LED with order m_i [15].

$$\alpha_i = \frac{(m_i + 1) A \cos^{m_i}(\phi_i) \cos(\theta_i)}{2\pi d_i^2}, \tag{2}$$

where A is the area of the PD, ϕ_i, θ_i, and d_i represent the radiation angle, incidence angle and distance between the i-th transmitter and PD receiver, respectively. The i-th transmitted signal $s_i(l)$ with particular frequency f_i from the i-th LED can be regarded as a DC-biased windowed sinusoid waveform with a duration Γ as follows:

$$\begin{aligned} s_i(l) &= a(l) b_i(l) \\ &= a(l) + a(l) \cos(2\pi f_i l), \end{aligned} \tag{3}$$

where $b_i(l) = 1 + \cos(2\pi f_i l)$, $a(l)$ is a baseband component and the second term is a bandpass component centered at f_i.

Further, the vertical heights of all LED transmitters o_i, $(i = 1, 2, \cdots, N)$ are fixed and equivalent. The localization plane is equipped with a VLC receiver set as the horizontal axis plane, that is, the height of the VLC receiver can be regarded as $o = 0$. Hence, the distance between the i-th LED transmitter and the PD receiver can be calculated as:

$$d_i = \sqrt{\left((x_i - x)^2 + (y_i - y)^2 + (o_i - 0)^2\right)} = c\tau_i, \tag{4}$$

where c is the speed of light and τ_i is the time delay.

Based on the received signal $\gamma(l)$, we can calculate the fast Fourier transform (FFT) of $\gamma(l)$ as

$$Y_M(\omega) = \sum_{l=0}^{M-1} \gamma(l) e^{-j\omega l}, \tag{5}$$

where M is length of the FFT, and $\omega = 2\pi f$ is the analog frequency. Based on the Parseval's relation, the periodogram PSD estimate of $\gamma(l)$ is given by:

$$S(\omega) = \frac{1}{M} |Y_M(\omega)|^2. \tag{6}$$

Referring to [14], the peaks of $S(\omega)$ can indicate the average powers of the received signals at different frequencies. Thus, we can obtain the estimated RSS vector $\boldsymbol{r}$ by capturing the peaks of fixed frequency in $S(\omega)$ as:

$$\boldsymbol{r} = [S(\omega_1), S(\omega_2), \cdots, S(\omega_N)]^T, \tag{7}$$

where $\omega_i = 2\pi f_i$ with f_i being the i-th frequency.

B. LOCALIZATION FRAMEWORK

In this paper, we study the fusion efficiency of multiple fingerprints/algorithms and apply FP to solve the problem of two-layer fusion for VLC-based localization. The proposed fusion scheme harnesses the complementary advantages exhibited by fusing diverse fingerprints as well as different classifiers. Unlike [14], we utilize the combination of multiple fingerprints to mitigate the fluctuation of RSS. We also weigh the various predictions from multiple algorithms to derive a more accurate localization estimate.

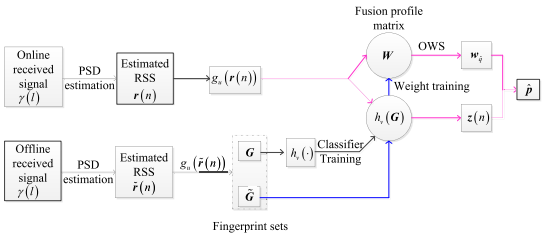

FIGURE 2. Overview of the proposed localization framework.

The implementation process of our proposed TLFN positioning algorithm is depicted in Fig. 2. Suppose that a location area is divided into Q grid points, each grid is numbered by a label q, $(q = 1, 2, \cdots, Q)$ and the area is covered by N LED transmitters. In the offline phase, the proposed algorithm involves three operations: 1) Derive two other fingerprints DIFF and HLF from the estimated RSS using the fingerprint function $g_u(\cdot)$, $(u = 1, 2, \cdots, U)$ to form the fingerprints sets (FSs), and divide the FSs into two groups, namely, $\boldsymbol{G} = [\boldsymbol{F}_{RSS}, \boldsymbol{F}_{DIFF}, \boldsymbol{F}_{HLF}]$ and $\tilde{\boldsymbol{G}} = \left[\tilde{\boldsymbol{F}}_{RSS}, \tilde{\boldsymbol{F}}_{DIFF}, \tilde{\boldsymbol{F}}_{HLF}\right]$; 2) Build multiple classifiers models $h_v(\boldsymbol{G})$, $(v = 1, 2, \cdots, V)$ by using the offline training set $\boldsymbol{G}$, where each classifier $h_v(\boldsymbol{G})$ maps from a fingerprint vector to a corresponding grid label; 3) Calculate the fusion profile (FP) matrix $\boldsymbol{W}$ using another set $\tilde{\boldsymbol{G}}$. Note that, $\boldsymbol{W}$ stores the weights of

different positioning estimation modalities at different grids and can be expressed as

$$\boldsymbol{W} = \left[\boldsymbol{w}_1, \boldsymbol{w}_2, \cdots, \boldsymbol{w}_Q\right]^T, \tag{8}$$

where $\boldsymbol{w}_q = \left[w_{q1}, w_{q2}, \cdots, w_{qT}\right]^T$ $(T = U \times V)$. FP can harness the complementary advantages between multiple algorithms and diverse fingerprints in a more refined perspective. In the online phase, given a testing RSS vector $\boldsymbol{r}(n)$ collected at an unknown location $\boldsymbol{p} = [x, y]^T$, we can obtain a FS by different fingerprint transformations $g_u(\cdot)$. After having constructed the FSs, the trained classifiers $h_v(\boldsymbol{G})$ are utilized to derive different location estimations. We then select the $\hat{q}$-th weight vector from $\boldsymbol{W}$ using our proposed OWS algorithm. The final location estimate $\hat{\boldsymbol{p}} = \left[\hat{x}, \hat{y}\right]^T$ is written as

$$\hat{\boldsymbol{p}} = \boldsymbol{w}_{\hat{q}}^T \boldsymbol{z}(n), \tag{9}$$

where $\boldsymbol{z}(n) = [z_1(n), z_2(n), \cdots, z_T(n)]^T$ and $z_t(n)$ is given by

$$z_t(n) = \rho\left(h_v\left(g_u\left(\boldsymbol{r}(n)\right), \boldsymbol{G}\right)\right), \tag{10}$$

in which $\rho(\cdot)$ is a transformation function $\Re^1 \rightarrow \Re^2$ maps a grid label to a 2-D coordinate. The proposed localization scheme implements the multi-layer fusion including fingerprints and classifiers, and more details about the TLFN-based positioning is analyzed in the next section.

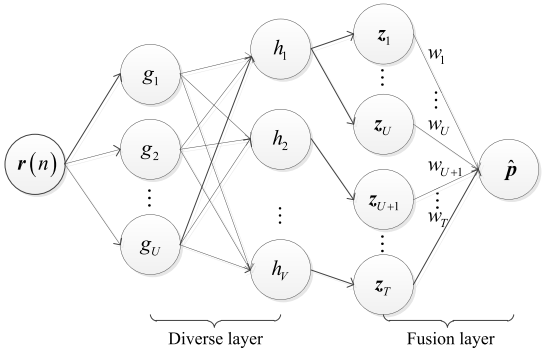

FIGURE 3. The two-layer fusion network architecture.

IV. PROPOSED ALGORITHM

We deploy our proposed fusion-based algorithm as a two-layer network as shown in Fig. 3. TLFN consists of a diverse layer [19] and a fusion layer. To localize a new received signal, the diverse layer can be used to obtain diversified location estimates. The fusion layer then weighs and combines the different estimates to yield a final location estimate.

A. DIVERSE LAYER

In the diverse layer, we first extract different kinds of fingerprints from the PSD vector to build fingerprints-based layer (FBL). Then each classifier in the classifiers-based layer (CBL) utilizes their local knowledge independently to produce a position estimate. By virtue of the diverse layer, the fingerprints in the fingerprints-based layer describe an indoor environment from different perspective. Also, the classifiers in the classifiers-based layer compensates the weakness of each other, i.e, they supplement each other. The diversified location estimates can be derived from the diverse layer, which provides the possibility of yielding more accurate localization results by properly combining those estimates together.

1) FINGERPRINTS-BASED LAYER (FBL)

The fingerprints-based fusion first proposed in [17], was implemented by utilizing received signals of multiple antennas. The authors further proposed a WiFi-based fingerprints fusion in [4] which included RSS, SSD and HLF to mitigate the hardware heterogeneity hurdle [17]. In this paper, considering the fingerprints efficiency in VLC systems and the computation complexity of the proposed algorithm, we adopt three different types of fingerprints (RSS, DIFF and HLF) to construct our fingerprints-based layer.

a: RSS

One of the most prevalent parameters employed in fingerprint localization for VLC-based system is RSS, since it doesn't require auxiliary devices compared to other fingerprints. As indicated earlier, the peaks of $S(\omega)$ denote the average powers of the received signal at different frequencies. Hence, it is rational to construct RSS fingerprints by extracting the peaks of PSD sequence. We denote $g_1(\cdot)$ as the RSS function, i.e.,

$$g_1(\boldsymbol{r}) = [S(\omega_1), S(\omega_2), \cdots, S(\omega_N)]^T. \tag{11}$$

Hence, the J RSS samples collected at the q-th grid, namely, $\boldsymbol{F}_{RSS}^q$, can be expressed as:

$$\boldsymbol{F}_{RSS}^q = \left[g_1\left(\boldsymbol{r}_q(1)\right), g_1\left(\boldsymbol{r}_q(2)\right), \cdots, g_1\left(\boldsymbol{r}_q(J)\right)\right]^T, \tag{12}$$

where $\boldsymbol{r}_q(j)$ represents the j-th RSS vector collected at the q-th grid point, J is the number of RSS samples collected from a particular grid. Thus, the RSS fingerprints subset for classifiers training can be expressed as $\boldsymbol{F}_{RSS} = \left[\boldsymbol{F}_{RSS}^1, \boldsymbol{F}_{RSS}^2, \cdots, \boldsymbol{F}_{RSS}^Q\right]^T \in \Re^{N \times J \times Q}$. We also denote $\tilde{\boldsymbol{F}}_{RSS}^q$ as the K RSS samples collected at the q-th grid point, expressed as:

$$\tilde{\boldsymbol{F}}_{RSS}^q = \left[g_1\left(\boldsymbol{r}_q(J+1)\right), g_1\left(\boldsymbol{r}_q(J+2)\right), \cdots, g_1\left(\boldsymbol{r}_q(J+K)\right)\right]^T. \tag{13}$$

Hence, the RSS fingerprints used for the fusion layer construction can be denoted as $\tilde{\boldsymbol{F}}_{RSS} = \left[\tilde{\boldsymbol{F}}_{RSS}^1, \tilde{\boldsymbol{F}}_{RSS}^2, \cdots, \tilde{\boldsymbol{F}}_{RSS}^Q\right]^T \in \Re^{N \times K \times Q}$.

b: DIFF

DIFF [24] was proposed as a more robust location fingerprint to yield more accurate and stable localization results than RSS fingerprints. DIFF is extrapolated by the differences between pairs of signal strength values to mitigate the impact

of heterogeneous devices. Although $\boldsymbol{r}$ is an approximation of RSS, we can also obtain the approximated DIFF based on the idea in [24]. Let $g_2(\cdot)$ be the DIFF function, DIFF can be expressed as:

$$g_2(\boldsymbol{r}) = \Delta S(\omega_{ij}) = S(\omega_i) - S(\omega_j), \tag{14}$$

where the indexes $i = 1, 2, \cdots, N-1$, $j = 2, 3, \cdots, N$; $i < j$, and a DIFF vector has C_2^N terms. Note that DIFF increases the dimensions from N to C_2^N as compared to RSS. Based on Eq. (14), we can also obtain two DIFF fingerprints training set: $\boldsymbol{F}_{DIFF} \in \Re^{J \times C_2^N \times Q}$ for classifier training and $\tilde{\boldsymbol{F}}_{DIFF} \in \Re^{K \times C_2^N \times Q}$ for fusion layer construction The formulations are given by:

$$\begin{aligned} \boldsymbol{F}_{DIFF} &= \left[\boldsymbol{F}^1_{DIFF}, \boldsymbol{F}^2_{DIFF}, \cdots, \boldsymbol{F}^Q_{DIFF}\right]^T, \\ \tilde{\boldsymbol{F}}_{DIFF} &= \left[\tilde{\boldsymbol{F}}^1_{DIFF}, \tilde{\boldsymbol{F}}^2_{DIFF}, \cdots, \tilde{\boldsymbol{F}}^Q_{DIFF}\right]^T, \end{aligned} \tag{15}$$

where the submatrix for each can be expressed respectively as, $\boldsymbol{F}^q_{DIFF} = \left[g_2\left(\boldsymbol{r}_q(1)\right), g_2\left(\boldsymbol{r}_q(2)\right), \cdots, g_2\left(\boldsymbol{r}_q(J)\right)\right]^T$ and $\tilde{\boldsymbol{F}}^q_{DIFF} = \left[g_2\left(\boldsymbol{r}_q(J+1)\right), g_2\left(\boldsymbol{r}_q(J+2)\right), \cdots, g_2(\boldsymbol{r}_q(J+K))\right]^T$. The DIFF fingerprints can reduce the hardware difference among LED transmitters since it has smaller variances than RSS fingerprints.

Note that both DIFF and SSD [22] consider signal strength difference as fingerprint features. However, we adopt DIFF instead of SSD, because SSD depends on the assumption of independence between transmitters.

c: HLF

HLF was derived by the signal strength ratios between pairs of base stations [21], which can mitigate the hardware variance problem without requiring extra manual calibration. Let $g_3(\cdot)$ be the HLF function, which can be expressed as:

$$g_3(\boldsymbol{r}) = \log\left(\frac{\zeta(i)}{\zeta(j)}\right) - \log\left(\frac{1}{\zeta_{\max}}\right), \tag{16}$$

where the indexes $i = 1, 2, \cdots, N-1$, $j = 2, 3, \cdots, N$; $i < j$, $\zeta(i) = S(\omega_i) + 225$ represents the converted term of $S(\omega_i)$, and $\zeta_{\max} = \max\{\zeta(1), \zeta(2), \cdots, \zeta(N)\}$. $\zeta(i)$ maps the PSD value to the integer scale $[0, 1, \cdots, 255]$ and it breaks the limitation of most signal-strength values represented as dBm values with different granularity.

Based on Eq. (16), we can obtain the submatrix $\boldsymbol{F}^q_{HLF}$ collected at the q-th grid point as:

$$\boldsymbol{F}^q_{HLF} = \left[g_3\left(\boldsymbol{r}_q(1)\right), g_3\left(\boldsymbol{r}_q(2)\right), \cdots, g_3\left(\boldsymbol{r}_q(J)\right)\right]^T, \tag{17}$$

Similarly, $\tilde{\boldsymbol{F}}^q_{HLF}$ is given by

$$\tilde{\boldsymbol{F}}^q_{HLF} = \left[g_3\left(\boldsymbol{r}_q(J+1)\right), g_3\left(\boldsymbol{r}_q(J+2)\right), \cdots, g_3\left(\boldsymbol{r}_q(J+K)\right)\right]^T. \tag{18}$$

Then the HLF fingerprints for classifiers training at all grid points can be expressed as $\boldsymbol{F}_{HLF} = \left[\boldsymbol{F}^1_{HLF}, \boldsymbol{F}^2_{HLF}, \cdots, \boldsymbol{F}^Q_{HLF}\right]^T \in \Re^{J \times C_2^N \times Q}$, and the other HLF fingerprints $\tilde{\boldsymbol{F}}_{HLF} = \left[\tilde{\boldsymbol{F}}^1_{HLF}, \tilde{\boldsymbol{F}}^2_{HLF}, \cdots, \tilde{\boldsymbol{F}}^Q_{HLF}\right]^T \in \Re^{K \times C_2^N \times Q}$ are used for fusion layer construction.

The construction process of the FBL is included in the diverse layer of our proposed TLFN-based localization scheme. Note that, unlike conventional techniques which utilize a single feature extraction like [16] to form a novel fingerprint, we regard U kinds of fingerprints as U types of location features, where each fingerprint serves as input to localization algorithms to produce independent location estimate. Note that we only consider three different kinds of fingerprints here, i.e., RSS, DIFF, and HLF, so the number of different kinds of fingerprints should be three, i.e., $U = 3$.

2) CLASSIFIERS-BASED LAYER (CBL)

As mentioned above, $h_v(\cdot)$ represents a classifier function, which maps a fingerprint vector into a corresponding location label (grid or coordinates). There are many candidates of $h_v(\cdot)$, roughly categorized into two: probabilistic algorithms and machine learning algorithms [25]. Probabilistic methods use statistical inference between the target signal measurement and the stored fingerprints, which mainly include Bayesian Network, Kullback-Leibler divergence, conditional random field, etc. Machine learning methods adopt a similarity metric to differentiate online signal measurement and fingerprint data, like KNN [26], support vector machine, random forest (RF) [27], extreme learning machine (ELM) [28], etc.

The CBL makes use of the phenomenon that any fingerprint positioning method has its characteristics. The performance of those approaches varies from inputs, environment and some dynamic factors. From heuristics obtained from [5], any classifier embraced in CBL can contribute to the final location estimate in a certain degree regardless of its accuracy. However, the basic criterion in selecting classifier functions is to meet good diversities and low average generalization error among fingerprint functions. Considering the real-time ability of inferring the user's coordinates in the online phase utilizing machine learning algorithms, we select three typical algorithms, KNN, RF and ELM to implement CBL, i.e., $V = 3$.

Given a training sample $\tilde{\boldsymbol{r}}(n)$ collected from the q-th grid point and the trained classifiers $h_v(\boldsymbol{G})$, we can obtain T estimates via U fingerprints and V classifiers, where $T = U \times V$. Let $\tilde{e}^q_t(n)$ be the t-th ($t = 1, 2, \cdots, T$) estimated label of the n-th sample collected at the q-th grid. For a refined metric required in the later stage, we set $\rho(\cdot)$ as a mapping function $\Re^1 \rightarrow \Re^2$, which converts a $1-D$ grid label $\tilde{e}^q_t(n)$ to a $2-D$ coordinate $\tilde{\boldsymbol{z}}^q_t(n)$. So the outputs of the diverse layer can be expressed as:

$$\tilde{\boldsymbol{z}}^q(n) = \left[\tilde{\boldsymbol{z}}^q_1(n), \tilde{\boldsymbol{z}}^q_2(n), \cdots, \hat{\boldsymbol{z}}^q_T(n)\right]^T, \tag{19}$$

where $\tilde{\boldsymbol{z}}^q_t(n) = \rho\left(\tilde{e}^q_t(n)\right)$ and $\tilde{e}^q_t(n)$ is given by

$$\tilde{e}^q_t(n) = h_v\left(g_u\left(\tilde{\boldsymbol{r}}(n)\right), \boldsymbol{G}\right). \tag{20}$$

B. FUSION LAYER

The aim of the fusion layer is to combine the multiple estimates from the diverse layer. We proposed an efficient fusion framework, GFP in [4] and [5], where we analyzed the superiority of GFP over the exiting fusion-based methods in WiFi-based localization. However, the GFPs in [4] and [5] are designed either for fingerprint-level fusion or algorithm-level fusion, which shows the limited fusion ability in accuracy improvement. In this paper, our FP is constructed for multiple fingerprints and multiple algorithm, which can offer a bigger fusion space than the GFPs in [4] and [5].

1) FP CONSTRUCTION

In the offline phase, in addition to building the two-layer fusion network, we further train a FP $\boldsymbol{W} \in \Re^{Q\times T}$ using $\tilde{\boldsymbol{G}}$. Note that the q-th row in the FP matrix $\boldsymbol{W}$, given by (8), denotes the weight vector of the q-th grid point, hence, we can train each row of the $\boldsymbol{W}$ sequentially by minimizing the average positioning errors as follows

$$\begin{aligned}\hat{\boldsymbol{w}}_q = \arg\min_{\boldsymbol{w}_q} \frac{1}{K}\sum_{n=J+1}^{J+K} \delta\left(\tilde{\boldsymbol{z}}^q(n)\,|\boldsymbol{w}_q\right)\\ s.t.\ \boldsymbol{w}_q^T\mathbf{1} = 1\\ w_{qt} \geq 0, \quad t = 1, 2, \cdots, T,\end{aligned} \tag{21}$$

where $\boldsymbol{w}_q^T\mathbf{1} = 1, q = 1, 2, \cdots, Q$ is a weight constraint which normalizes all the weights in the same scale and $\mathbf{1}$ is $T \times 1$ all one vector. And $\delta\left(\tilde{\boldsymbol{z}}^q(n)\,|\boldsymbol{w}_q\right)$ is the error function of all estimated results at the q-th grid, i.e.,

$$\delta\left(\tilde{\boldsymbol{z}}^q(n)\,|\boldsymbol{w}_q\right) = \|\boldsymbol{w}_q^T\tilde{\boldsymbol{z}}^q(n) - \boldsymbol{p}_q\|_2, \tag{22}$$

where $\|\cdot\|_2$ is the ℓ_2-norm. Apparently, FP can yield a more accurate positioning by weighing the intrinsic correlation among multiple location estimates. By solving the nonlinear optimization problem for all Q grid points, as depicted in Eq. (21), we can obtain Q vectors of length T. We summarize the procedures of FP construction in Algorithm 1.

2) OWS

Given an online testing sample $\boldsymbol{r}(n)$, searching for the optimal weights, $\boldsymbol{w}_q$ in the proposed FP is another key problem for fusion efficiency. We propose an intelligent weight searching strategy by resorting to the outputs from the diverse layer, i.e., an appropriate weight $\boldsymbol{w}_q$, for the grid index q for $\boldsymbol{r}(n)$ can be obtained via leveraging all location estimates. This search strategy first finds the optimal estimator using the training localization estimates $\tilde{\boldsymbol{z}}^q(n)$.

$$\hat{t} = \arg\min_{t} \sum_{q=1}^{Q}\sum_{n=J+1}^{J+K} \|\tilde{\boldsymbol{z}}_t^q(n) - \boldsymbol{p}_q\|_2. \tag{23}$$

With the optimal estimator's index in Eq. (23), we then heuristically find a suitable grid index q by comparing the online estimates $\boldsymbol{z}_{\hat{t}}(n)$ and the stored estimates $\tilde{\boldsymbol{z}}_{\hat{t}}^q(n)$ in the offline phase, where $\boldsymbol{z}_{\hat{t}}(n)$ is a particular term from $\boldsymbol{z}(n)$ generated by the diverse layer for $\boldsymbol{r}(n)$, and $\tilde{\boldsymbol{z}}_{\hat{t}}^q(n) \in \tilde{\boldsymbol{z}}^q(n)$.

$$\hat{q} = \arg\min_{q} \sum_{q=1}^{Q} \|\boldsymbol{z}_{\hat{t}}(n) - \tilde{\boldsymbol{z}}_{\hat{t}}^q(n)\|_2. \tag{24}$$

According to the grid index $\hat{q}$, we can determine the weight $\boldsymbol{w}_{\hat{q}}$ from the FP. The final location result can be computed using Eq. (9). Note that, OWS strategy is based on the outputs from TLFN instead of directly matching the data distribution, which efficiently mitigates the fluctuation of received signals. We summarize the procedures of weights selection of TLFN-based positioning scheme in Algorithm 2.

Algorithm 1 FP Construction

Input: 1) The training RSS vector $\tilde{\boldsymbol{r}}(n)$ 2) The number of grid points Q 3) The number of fingerprint functions U 4) The number of classifiers V
Output: The FP matrix $\boldsymbol{W}$

```
for u = 1, 2, ··· , U do
    Define the fingerprints g_u(·) using Eqs. (12), (14), and (17) in the FBL
end for
Generate the FSs G, G̃
for v = 1, 2, ··· , V do
    Train the classifier h_v(g_u(r̃(n))) using G
end for
Generate the CBL
for q = 1, 2, ··· , Q do
    for n = J + 1, J + 2, ··· , J + K do
        Compute the diverse layer outputs z̃^q(n) using Eq. (19)
        Compute the localization error δ(z̃^q(n) | w_q) using Eq. (22)
    end for
    Compute the weighs at the q-th grid ŵ_q using Eq. (21)
end for
Ŵ = [ŵ_1, ŵ_2, ··· , ŵ_Q]^T
return Ŵ
```

Algorithm 2 OWS

Input: 1) The online testing RSS vector $\boldsymbol{r}(n)$ 2) $\tilde{\boldsymbol{G}}$ 3) The trained CBL
Output: The optimal weights $\boldsymbol{w}_{\hat{q}}$

```
for t = 1, 2, ··· , T do
    Compute the diverse layer outputs z_t(n) using Eq. (19)
end for
Find the optimal estimator index t̂ using Eq. (23)
Estimate the matched grid point q̂ using Eq. (24)
return w_q̂
```

C. PERFORMANCE ANALYSIS

1) ACCURACY

With TLFN juxtaposed with existing fusion methods, we analyze two factors that can guarantee accuracy amelioration

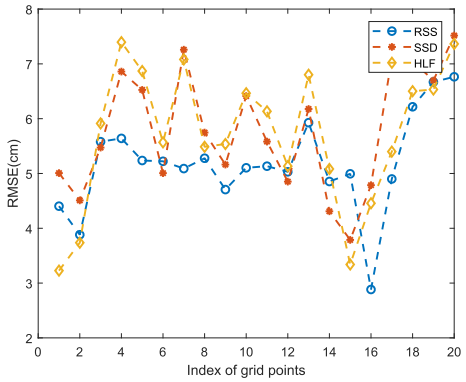

FIGURE 4. Fingerprints diversity.

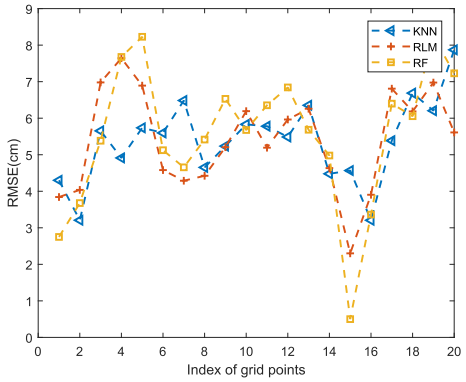

FIGURE 5. Classifiers diversity.

of our proposed fusion-based localization framework. First, the diverse layer can improve the performance of our localization system by compensating for the fluctuation of RSS in the FBL, and also via combining the complementary advantages among the CBL. Secondly, Fig. 4 illustrates the positioning errors based on multiple fingerprints with the same classifier, while Fig. 5 shows the positioning errors by using multiple classifiers with the same fingerprint. This two Figures prove that, these diverse estimates provide a possibility to tweak or refine localization accuracy. Also, our proposed fusion layer can fully excavate the intrinsic supplementation among different location estimates. More importantly, the superiority of our proposed TLFN in terms of localization accuracy will not diminish with respect to complex or dynamic environments. More experimental details are expounded in Section V.

2) ROBUSTNESS

The robustness of our proposed fusion localization framework is analyzed from the following aspects: Firstly, the fingerprints utilized in this paper, i.e, RSS, DIFF and HLF have different intrinsic characteristics. HLF takes ratios of RSS values between pairs of PSDs as fingerprint features, which can lessen the repercussions of varying transmitter power. While DIFF calculates the signal difference between all transmitters. This means DIFF and HLF can handle the power differences among transmitters.

Secondly, we adopt three typical machine learning methods as classifiers instead of other trilateration methods. With respect to robustness or model training, machine learning methods have great preponderance in dealing with model error and fingerprints fluctuation. Finally, the proposed fusion layer implemented by constructing a FP to dynamically weigh multiple positioning models, instead of utilizing a single location estimate. Thus, our proposed TLFN can combine multiple positioning results, further ameliorating positioning robustness.

V. EXPERIMENTAL SETUP AND RESULTS

To evaluate the performance of this new fusion modus operandi, TLFN-based positioning, we juxtapose it with other typical fusion-based approaches including GILS [14], FAGOT [4], KAAL [5], MMSE [18] and DFC [23]. We adopt the RMSE as the error metric because it accumulatively gives a reasonable estimate of the error. The root mean square error (RMSE) is defined as:

$$RMSE = \sqrt{\frac{1}{\mathcal{I}}\sum_{i=1}^{\mathcal{I}}\left[\left(\hat{x}_i - x\right)^2 + \left(\hat{y}_i - y\right)^2\right]} \tag{25}$$

where $\left[\hat{x}_i, \hat{y}_i\right]^T$ stands for the i-th location estimate, $[x_i, y_i]^T$ represents the true location, and $\mathcal{I}$ is the number of experimental trials.

A. EXPERIMENTAL SETUP

The experimental setup to be utilized to test our proposed TLFN algorithm in this paper is a testbed built in the optimized networking laboratory, which is located on the fourth floor of the Faculty Memorial Hall building of New Jersey Institute of Technology. Our proposed localization system is depicted in Fig. 7, the signal transmission is implemented by two Universal Software Radio Peripheral (USRPs) N210 equipped with LFTX daughterboards to drive the light sources, and one USRP N120 with LFRX daughterboard used as a signal receiver. An avalanche photo detector APD 130 A2/M from Thorlabs is utilized to implement the conversion from optical to electrical. Specifically, we transfer four sinusoidal signals with different frequencies (these are 800kHz, 850kHz, 900kHz and 950kHz, respectively) generated from GNU Radio via USRPs. A combination of sinusoidal signals with 23.6 Volts DC power supplied by 4 Bias tees- ZFBT-6GW+, is used as the driving source for the four visible lights. The photo dioxide receives the transmitted signals and forwards the signals to the USRP for signal extraction.

The testbed is about 0.7m×0.7m with four visible light sources ($N = 4$), where each light source consists of two premium daylight white LED arrays from Solid Apollo LED as shown in Fig. 6. Specifically, we divide the experimental testbed into $Q = 225$ grids and the distance between two neighboring grids is 5cm. We take the location plane coordinate where the fist grid is to serve as the origin. The locations of the four sparsely deployed

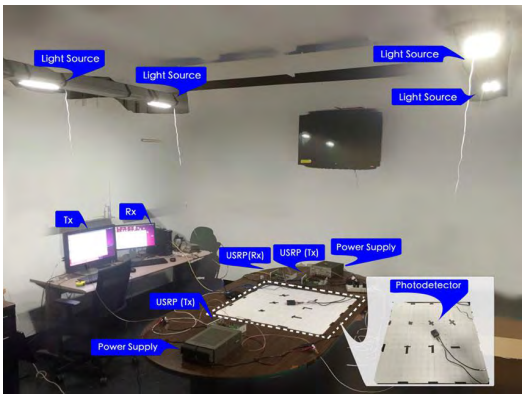

FIGURE 6. Testbed in our experimental study.

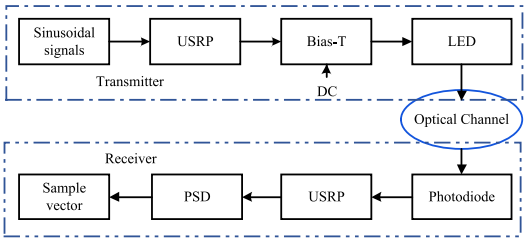

FIGURE 7. The block diagram of our proposed localization system.

LEDs are $\boldsymbol{p}_1 = [-1, 13m, -0.67m, 1.48m]^T$, $\boldsymbol{p}_2 = [1.56m, -0.7m, 1.48m]^T$, $\boldsymbol{p}_3 = [-1, 13m, 0.5m, 1.48m]$, $\boldsymbol{p}_4 = [1.56m, 0.47m, 1.48m]^T$ (In fact, our method does not need to know the coordinates of the four transmitters). The signal strength can be extracted to construct a sample vector using Eq. (7), where each location is recoded for 5 seconds, the sampling rate is set to 4 MHz and the length of FFT $M = 2048$. Note that, the amplitude of the sinusoidal signal is not fixed and fluctuates from 0 to 1, which results in the uncertainty of signals received.

Two FSs $\boldsymbol{G}$ and $\tilde{\boldsymbol{G}}$ with $J = 120$ and $K = 40$ training samples at each grid, respectively. $\boldsymbol{G}$ is used to build the CBL, and $\tilde{\boldsymbol{G}}$ is utilized to construct the FP utilizing Algorithm 1. In the online phase, we collect 225×40 samples from the whole testbed area to evaluate the performance of our proposed TLFN-based positioning technique.

B. FUSION NECESSITY ANALYSIS

Fusion of multiple information, instead of utilizing a single classifier or fingerprint is a propitious strategy in enhancing localization accuracy. However the fusion strategy of some existing fusion methods, such as dynamic fusion combination method (DFC) [23], cannot fully leverage the diversity of the fusion sources, thus showing limited improvement in positioning accuracy. To demonstrate the weight assigning strategy of our proposed VLC-based localization, we show the weights assigned to each fingerprint-classifier combination for the first 10 grids because of limited space. The performance difference among multiple fingerprint-classifier pairs is clearly depicted in Fig. 8. Each fingerprint/classifier

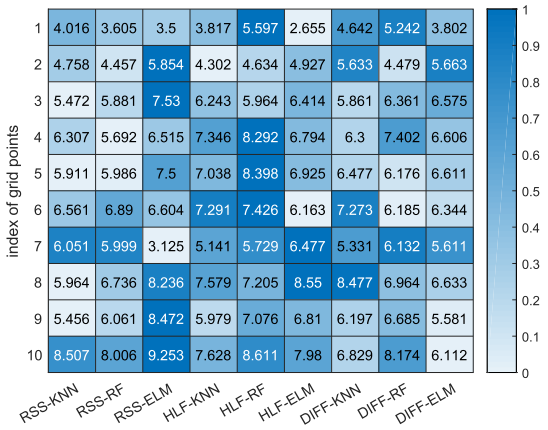

FIGURE 8. The positioning errors of fingerprint-classifier combinations.

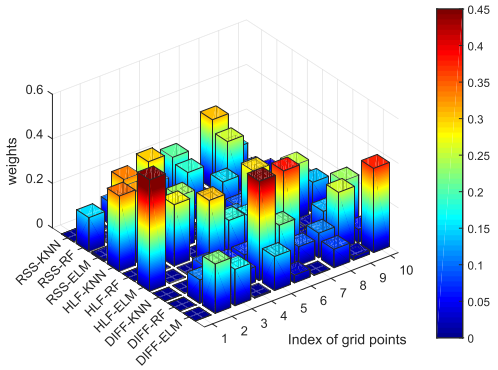

FIGURE 9. Fusion weights of our proposed TLFN.

has its characteristics at different grids. This explains why we introduced the diverse layer to enhance positioning accuracy. Our proposed TLFN achieves this goal by dynamically combining multi-mode outputs from the diverse layer, in other words, our method can obtain the optimal estimation by searching the weights in the bigger fingerprint and algorithm space. Fig. 9 gives a more pictorial representation of the different weight profiles of our proposed TLFN algorithm. It shows the weight estimates from the diverse layer and it also shows the weights assigned are unique for each grid. To be laconic, dynamic weighing among the classifiers reflects the differences in performance among fused estimations. This proves that our fusion layer in the TLFN can fully excavate the complementary advantages of multiple results.

C. COMPARATIVE ANALYSIS

To manifest the efficiency of TLFN, we juxtapose it with various fingerprint-classifier combinations as well as other fusion-based methods. As depicted in Fig. 10, TLFN surpasses all successive fingerprint-classifier pairs. Note that any number or choice of classifiers can be selected to implement our proposed modus operandi. Each fingerprint-classifier pair has its unique characteristics and their amalgamation yields far better results than utilizing single positioning models.

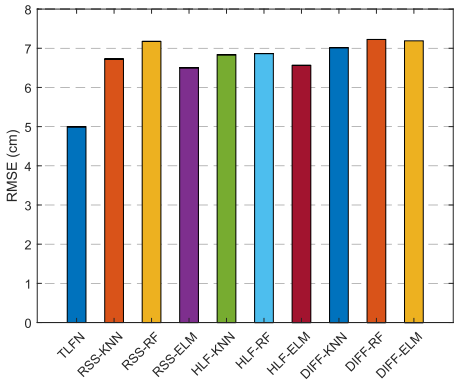

FIGURE 10. The RMSEs of fingerprint-classifier combinations compared with TLFN.

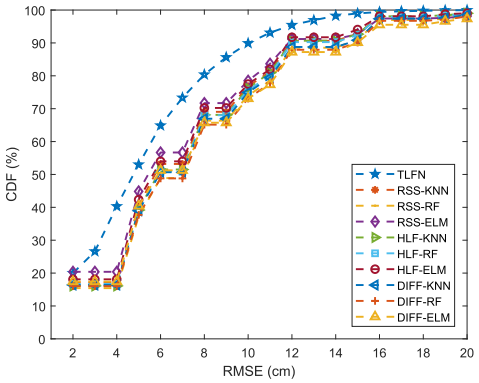

FIGURE 11. CDF of fingerprint-classifier combinations juxtaposed with TLFN.

We also illustrate the CDF of various fingerprint-classifier combinations with TLFN in Fig. 11. It's notable that TLFN reduces the 90th percentile by 13.19%, 16.02%, 13.53%, 13.8%, 14.43%, 12.25%, 15.08%, 16.94% and 19.44% of RSS-KNN, RSS-RF, ESS-ELM, HLF-KNN, HLF-RF, HLF-ELM, DIFF-KNN, DIFF-RF and DIFF-ELM respectively. This improvement is attributed to the joint utilization of diverse layer and fusion layer.

Further to clarify the merits of TLFN, we compare it with other extant fusion methods such as GILS [14], FAGOT [4], KAAL [5], MMSE [18], and DFC [23]. The RMSEs of these fusion-based methods compared with TLFN are presented in Fig. 12. The RMSEs of GILS, FAGOT, KAAL, MMSE and DFC are 5.36, 5.31, 5.43, 5.44 and 5.36 centimeters, respectively. DFC performs worst with a RMSE of 5.44 cm, this is because, DFC cannot fully harness the complementarity among different location estimates. Note that KAAL is the second-best fusion-based methods after TLFN, because it considers the diversities among the FBL. The RMSE of our proposed TLFN is 5cm, which outperforms other fusion methods. The experimental results show that our proposed TLFN can fully exploit the inherent supplementation among diverse location estimates, thus it realizes superior performance over the other tested methods. The more complex the

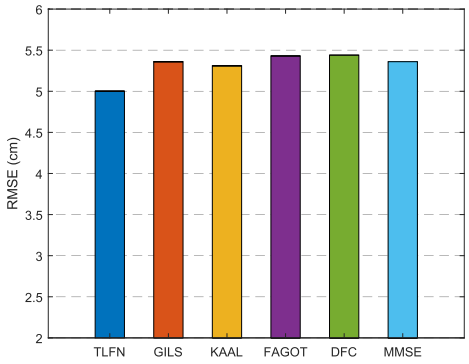

FIGURE 12. The RMSEs of fusion-based techniques compared with TLFN.

TABLE 1. CDF comparisons of fusion-based methods.

Methods	50^{th} percentile	67^{th} percentile	90^{th} percentile	Average
TLFN	2.30	3.02	4.17	5.00
GILS	2.80	3.47	4.59	5.36
KAAL	2.36	3.12	4.40	5.31
FAGOT	2.70	3.40	4.58	5.43
DFC	2.85	3.53	4.65	5.44
MMSE	2.80	3.47	4.59	5.36

indoor environment is, the more superior our proposed algorithm. For clearer and more intuitive analysis, TABLE 1 provides the CDF values of the RMSEs. It is shown that TLFN can improve the accuracy of localization without increasing the complexity.

VI. CONCLUSION

In this paper, we propose a TLFN-based scheme for VLC-based indoor positioning system. We first generate a diverse layer via amalgamating multiple fingerprints and multiple classifiers to obtain various localization estimates to mitigate the signal inaccuracies caused by the instability and uncertainty of the LED transmitters. Then, in the offline stage, we train a FP to store the weights of all estimated modalities via minimizing the average localization error. In the online stage, we design an OWS strategy to find the appropriate weights from the FP matrix. Considering the complementary information between the FBL and the CBL, our proposed localization framework can derive a combined estimation that is more accurate and more stable than the estimation of any single positioning estimator.

REFERENCES

[1] J. Luo, L. Fan, and H. Li, "Indoor positioning systems based on visible light communication: State of the art," *IEEE Commun. Surveys Tuts.*, vol. 19, no. 4, pp. 2871–2893, 4th Quart., 2017.

[2] B. Molina, E. Olivares, C. E. Palau, and M. Esteve, "A multimodal fingerprint-based indoor positioning system for airports," *IEEE Access*, vol. 6, pp. 10092–10106, 2018.

[3] M. Ayyash *et al.*, "Coexistence of WiFi and LiFi toward 5G: Concepts, opportunities, and challenges," *IEEE Commun. Mag.*, vol. 54, no. 2, pp. 64–71, Feb. 2016.

[4] X. Guo, L. Li, N. Ansari, and B. Liao, "Accurate WiFi localization by fusing a group of fingerprints via a global fusion profile," *IEEE Trans. Veh. Technol.*, vol. 67, no. 8, pp. 7314–7325, Aug. 2018.

[5] X. Guo, L. Li, N. Ansari, and B. Liao, "Knowledge aided adaptive localization via global fusion profile," *IEEE Internet Things J.*, vol. 5, no. 2, pp. 1081–1089, Apr. 2018.
[6] N. Hernaindez, J. M. Alonso, and M. Ocaa, "Fuzzy classifier ensembles for hierarchical WiFi-based semantic indoor localization," *Expert Syst. Appl.*, vol. 90, pp. 394–404, Dec. 2017.
[7] M. F. Keskin, A. D. Sezer, and S. Gezici, "Localization via visible light systems," *Proc. IEEE*, vol. 106, no. 6, pp. 1063–1088, Jun. 2018.
[8] W. Guan *et al.*, "A novel three-dimensional indoor positioning algorithm design based on visible light communication," *Opt. Commun.*, vol. 392, pp. 282–293, Jun. 2017.
[9] Y. Wu, X. Liu, W. Guan, B. Chen, X. Chen, and C. Xie, "High-speed 3D indoor localization system based on visible light communication using differential evolution algorithm," *Opt. Commun.*, vol. 424, pp. 177–189, Oct. 2018.
[10] T. Q. Wang, Y. A. Sekercioglu, A. Neild, and J. Armstrong, "Position accuracy of time-of-arrival based ranging using visible light with application in indoor localization systems," *J. Lightw. Technol.*, vol. 31, no. 20, pp. 3302–3308, Oct. 15, 2013.
[11] M. F. Keskin, S. Gezici, and O. Arikan, "Direct and two-step positioning in visible light systems," *IEEE Trans. Commun.*, vol. 66, no. 1, pp. 239–254, Jan. 2018.
[12] S.-Y. Jung, S. Hann, and C.-S. Park, "TDOA-based optical wireless indoor localization using LED ceiling lamps," *IEEE Trans. Consum. Electron.*, vol. 57, no. 4, pp. 1592–1597, Nov. 2011.
[13] A. Arafa, S. Dalmiya, R. Klukas, and J. F. Holzman, "Angle-of-arrival reception for optical wireless location technology," *Opt. Express*, vol. 23, no. 6, pp. 7755–7766, 2015.
[14] X. Guo, S. Shao, N. Ansari, and A. Khreishah, "Indoor localization using visible light via fusion of multiple classifiers," *IEEE Photon. J.*, vol. 9, no. 6, Dec. 2017, Art. no. 7803716.
[15] H.-S. Kim, D.-R. Kim, S.-H. Yang, Y.-H. Son, and S.-K. Han, "An indoor visible light communication positioning system using a RF carrier allocation technique," *J. Lightw. Technol.*, vol. 31, no. 1, pp. 134–144, Jan. 1, 2013.
[16] S.-H. Fang and C.-H. Wang, "A novel fused positioning feature for handling heterogeneous hardware problem," *IEEE Trans. Commun.*, vol. 63, no. 7, pp. 2713–2723, Jul. 2015.
[17] X. Guo and N. Ansari, "Localization by fusing a group of fingerprints via multiple antennas in indoor environment," *IEEE Trans. Veh. Technol.*, vol. 66, no. 11, pp. 9904–9915, Nov. 2017.
[18] Y. Gwon, R. Jain, and T. Kawahara, "Robust indoor location estimation of stationary and mobile users," in *Proc. IEEE INFOCOM*, vol. 2, Mar. 2004, pp. 1032–1043.
[19] L. Wang and W.-C. Wong, "Fusion of multiple positioning algorithms," in *Proc. IEEE ICICS*, Dec. 2011, pp. 1–5.
[20] Y. Zhuang *et al.*, "A survey of positioning systems using visible LED lights," *IEEE Commun. Surveys Tuts.*, vol. 20, no. 3, pp. 1963–1988, 3rd Quart., 2018.
[21] M. B. Kjærgaard and C. V. Munk, "Hyperbolic location fingerprinting: A calibration-free solution for handling differences in signal strength (concise contribution)," in *Proc. IEEE PERCOM*, Mar. 2008, pp. 110–116.
[22] A. M. Hossain, H. N. Van, Y. Jin, and W.-S. Soh, "Indoor localization using multiple wireless technologies," in *Proc. IEEE MASS*, Oct. 2007, pp. 1–8.
[23] S.-H. Fang, Y.-T. Hsu, and W.-H. Kuo, "Dynamic fingerprinting combination for improved mobile localization," *IEEE Trans. Wireless Commun.*, vol. 10, no. 12, pp. 4018–4022, Dec. 2011.
[24] F. Dong, Y. Chen, J. Liu, Q. Ning, and S. Piao, "A calibration-free localization solution for handling signal strength variance," in *Mobile Entity Localization and Tracking in GPS-less Environnments*. Orlando, FL, USA: Springer, 2009, pp. 79–90.
[25] Z. Tian, X. Tang, M. Zhou, and Z. Tan, "Fingerprint indoor positioning algorithm based on affinity propagation clustering," *EURASIP J. Wireless Commun. Netw.*, vol. 2013, no. 1, p. 272, 2013.
[26] Y. Xie, Y. Wang, A. Nallanathan, and L. Wang, "An improved K-nearest-neighbor indoor localization method based on spearman distance," *IEEE Signal Process. Lett.*, vol. 23, no. 3, pp. 351–355, Mar. 2016.
[27] X. Guo, N. Ansari, L. Li, and H. Li, "Indoor localization by fusing a group of fingerprints based on random forests," *IEEE Internet Things J.*, vol. 5, no. 6, pp. 4686–4698, Dec. 2018.
[28] H. Zou, X. Lu, H. Jiang, and L. Xie, "A fast and precise indoor localization algorithm based on an Online sequential extreme learning machine," *Sensors*, vol. 15, no. 1, pp. 1804–1824, Jan. 2015.

XIANSHENG GUO (S'07–M'11) received the B.Eng. degree from Anhui Normal University, Wuhu, China, in 2002, the M.Eng. degree from the Southwest University of Science and Technology, Mianyang, China, in 2005, and the Ph.D. degree from the University of Electronic Science and Technology of China (UESTC), Chengdu, China, in 2008. From 2008 to 2009, he was a Research Associate with the Department of Electrical and Electronic Engineering, The University of Hong Kong. From 2012 to 2014, he was a Research Fellow with the Department of Electronic Engineering, Tsinghua University. From 2016 to 2017, he was a Research Scholar with the Advanced Networking Laboratory, Department of Electrical and Computer Engineering, New Jersey Institute of Technology, Newark, NJ, USA. He is currently an Associate Professor with the Department of Electronic Engineering, UESTC. His research interests include array signal processing, wireless localization, machine learning, information fusion, and software radio design.

FANGZI HU (S'13) received the B.Eng. degree from Yanbian University, Yanji, China, in 2017. She is currently pursuing the master's degree in information and communication engineering with the University of Electronic Science and Technology of China, Chengdu, China. Her current research interests include indoor localization, machine learning, and information fusion.

NKROW RAPHAEL ELIKPLIM received the B.Sc. degree in computer science from the Kwame Nkrumah University of Science and Technology, Ghana, in 2014. He is currently pursuing the master's degree in information and communication engineering with the University of Electronic Science and Technology of China, Chengdu, China.

He also has three years working experience in the telecommunication industry. His research interests include machine learning, information fusion, and indoor localization.

LIN LI (S'12) received the B.Eng. degree from the University of Electronic Science and Technology of China (UESTC), Chengdu, China, in 2016, where he is currently pursuing the Ph.D. degree with the Department of Information and Communication Engineering.

His research interests include indoor localization, machine learning, and transfer learning.